International Journal of Innovative
Computing, Information and Control
Volume **10**, Number **5**, October **2014**

ICIC International ©2014 ISSN 1349-4198
pp. 1791–1808

# AN INTELLIGENT SWITCHING OVERVOLTAGES ESTIMATOR FOR POWER SYSTEM RESTORATION USING ARTIFICIAL NEURAL NETWORK

Iman Sadeghkhani[1], Abbas Ketabi[2] and Rene Feuillet[3]

[1]Department of Electrical Engineering
Najafabad Branch, Islamic Azad University
Najafabad 85141-43131, Iran
i.sadeghkhani@ec.iut.ac.ir

[2]Department of Electrical Engineering
University of Kashan
Kashan 87317-51167, Iran
aketabi@kashanu.ac.ir

[3]Grenoble Electrical Engineering Lab (G2ELab)
Grenoble INP, France
rene.feuillet@g2elab.grenoble-inp.fr

Received December 2012; revised December 2013

Abstract. *One of the most important issues in power system restoration (PSR) is switching overvoltage caused by power equipment energization. This phenomenon may damage some equipment and delay power system restoration. This paper proposes an intelligent estimator which can be used to evaluate and control switching overvoltages. Transformer, shunt reactor, and transmission lines are important devices in PSR and their energization have been studied in this work. Artificial neural network (ANN) is adopted as an intelligent approach to deal with these overvoltages. Both Multilayer Perceptron (MLP) and Radial Basis Function (RBF) structures have been analyzed. Five learning algorithms, backpropagation (BP), delta-bar-delta (DBD), extended delta-bar-delta (EDBD), directed random search (DRS), and quick propagation (QP) were used to train the MLP. In the cases of transformer and shunt reactor energization, ANNs are trained with the worst case scenario of switching angle and remanent flux which reduce the number of required simulations for training ANN. Also, for achieving good generalization capability for developed ANN, equivalent parameters of the network are used as ANN inputs. The simulated results for a partial of 39-bus New England test system show that the proposed technique can estimate the peak values and duration of switching overvoltages with good accuracy and EDBD algorithm presents best performance.*
**Keywords:** Artificial neural networks, Harmonic index, Power system restoration, Power equipment energization, Switching overvoltages

1. **Introduction.** In recent years, due to economic competition and deregulation, power systems are being operated closer and closer to their limits. At the same time, power systems have increased in size and complexity. Both factors increase the risk of major power outages. After a blackout, power needs to be restored as quickly and reliably as possible and, consequently, detailed restoration plans are necessary [1,2]. If the frequency characteristic of the system shows resonance conditions around multiples of the fundamental frequency, very high and weakly damped temporary overvoltages (TOVs) of long duration may occur when the system is excited by a harmonic disturbance, such as the switching of lightly loaded transformers or transformer saturation [1,3-5].

One of the major concerns in power system restoration is the occurrence of overvoltages as a result of switching procedures. These can be classified as transient overvoltages, sustained overvoltages, harmonic resonance overvoltages, and overvoltages resulting from ferro-resonance. Steady-state overvoltages occur at the receiving end of lightly loaded transmission lines as a consequence of line-charging currents (reactive power balance). Excessive sustained overvoltages may lead to damage of transformers and other power system equipment. Transient overvoltages are a consequence of switching operations on long transmission lines, or the switching of capacitive devices, and may result in arrester failures. Ferro-resonance is a non-harmonic resonance characterized by overvoltages whose waveforms are highly distorted and can cause catastrophic equipment damages [1,6-9].

In [10], maximal voltages induced on overhead power lines by a nearby lightning stroke are estimated. In [11], a comparison is made between two coupling models frequently used to estimate the lightning-induced overvoltages in power lines. Also, in [12] fast transient overvoltage in gas-insulated substation is estimated. In [13], a qualitative method of prediction for voltages to the first peak value is provided, which is quantitative once the 'universal curve' (defined in the text) is known. In [14], an artificial neural network is trained to estimate peak overvoltage generated in presence of back flashover. Also, in [15] single-phase transmission line overvoltage peak is estimated by using artificial neural network (ANN). Moreover, the author evaluated single-phase transformer overvoltages using radial basis function (RBF) neural network in [16].

In this paper, switching overvoltages caused by transformer, shunt reactor, and transmission line energization are evaluated. In order to study temporary overvoltages for a large number of possible system configurations, it is necessary to run many time-domain simulations resulting in a large amount of simulation time. In transformer and shunt reactor energization study, a way to limit the overall calculation time is to reduce the number of simulations by applying analytical or knowledge-based rules to discard a number of system configurations before an actual time-domain simulation is carried out. This paper presents the artificial neural network (ANN) application for estimation of peak and duration overvoltages under switching transients during transformer, shunt reactor, and transmission lines energization. Moreover, in the ANN training process, equivalent parameters of the network are used; this causes developed ANN can be applied to every studied system. A tool such as the one proposed in this paper that can give the maximum switching overvoltage and its duration will be helpful to the operator during system restoration; since after a blackout, power needs to be restored as fast and reliable as possible. Because of ANN responses to its inputs real-time, operators can use it to select the best sequence of equipment energization. Also it can be used as a training tool for the operators. Results of the studies are presented for a partial of 39-bus New England test system to illustrate the proposed approach.

This paper is organized as follows. Section 2 presents the basic concepts of proposed ANN models. Section 3 proposes a training technique based on equivalent circuit parameters. Also, a new harmonic-index is introduced for transformer and shunt reactor energization to reduce the number of required simulations for training ANN. Section 4 presents the test cases and results. Discussion is reported in Section 5 and in Section 6, a conclusion will be drawn.

2. **The Artificial Neural Network.** There are many types of neural networks for various applications available in the literature [17-21]. Multilayer Perceptrons (MLPs) and Radial Basis Functions (RBFs) are examples of feed-forward networks and both universal approximators. In spite of being different networks in several important respects, these two neural network architectures are capable of accurately mimicking each other.

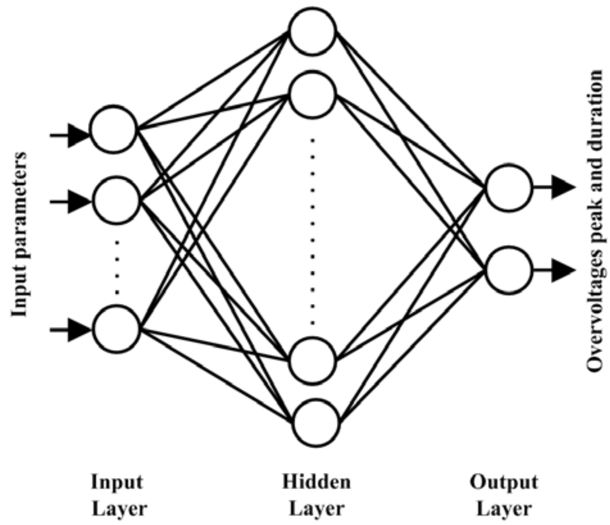


FIGURE 1. The structure of multilayer perceptron neural network

2.1. **Multilayer perceptrons (MLPs).** Multilayer perceptrons are the simplest and therefore most commonly used neural network architectures. The basic structure of the MLP is shown in Figure 1. The MLP consists of three layers namely, the input layer, the hidden layer, and the output layer. Training a network consists of adjusting weights of the network using a different learning algorithm. In this paper, backpropagation (BP), the delta-bar-delta (DBD), the extended delta-bar-delta (EDBD), the directed random search (DRS), and quick propagation (QP) were used to train the MLP. A learning algorithm gives the change $\Delta w_{ji}(k)$ in the weight of a connection between neurons $i$ and $j$. In the next section, these learning algorithms have been explained briefly.

2.1.1. *Backpropagation (BP) algorithm.* The BP with momentum [17] is the most commonly adopted MLP training algorithm. It is a gradient descent algorithm and gives the change $\Delta w_{ji}(k)$ in the weight of a connection between neurons $i$ and $j$ as follows:

$$\Delta w_{ji}(k) = \alpha\delta_j x_i + \mu\Delta w_{ji}(k-1) \tag{1}$$

where $x_i$ is the input, $\alpha$ is a parameter called the learning coefficient, $\mu$ is the momentum coefficient, and $\delta_j$ is a factor depending on whether neuron $j$ is an output neuron or a hidden neuron.

2.1.2. *Delta-Bar-Delta (DBD) algorithm.* The DBD algorithm is a heuristic approach to improve the convergence speed of the weights in ANNs [22]. The weights are updated by

$$w(k+1) = w(k) + \alpha(k)\delta(k) \tag{2}$$

where $\alpha(k)$ is the learning coefficient and assigned to each connection, $\delta(k)$ is the gradient component of the weight change. $\delta(k)$ is employed to implement the heuristic for incrementing and decrementing the learning coefficients for each connection. The weighted average $\bar{\delta}(k)$ is formed as

$$\bar{\delta}(k) = (1-\theta)\delta(k) + \theta\delta(k-1) \tag{3}$$

where $\theta$ is the convex weighting factor. The learning coefficient change is given as

$$\Delta\alpha(k) = \begin{cases} \kappa & \bar{\delta}(k-1)\delta(k) > 0 \\ -\varphi\alpha(k) & \bar{\delta}(k-1)\delta(k) < 0 \\ 0 & \text{otherwise} \end{cases} \tag{4}$$

where $\kappa$ is the constant learning coefficient increment factor, and $\varphi$ is the constant learning coefficient decrement factor.

2.1.3. *Extended Delta-Bar-Delta (EDBD) algorithm.* The EDBD algorithm is an extension of the DBD and based on decreasing the training time for ANNs [23]. In this algorithm, the changes in weights are calculated from:

$$\Delta w(k+1) = \alpha(k)\delta(k) + \mu(k)\Delta w(k) \tag{5}$$

and the weights are then found as

$$w(k+1) = w(k) + \Delta w(k) \tag{6}$$

In Equation (5), $\alpha(k)$ and $\mu(k)$ are the learning and momentum coefficients, respectively. The learning coefficient change is given as

$$\Delta\alpha(k) = \begin{cases} \kappa_a \exp(-\gamma_\alpha \left|\bar{\delta}(k)\right|) & \text{if } \bar{\delta}(k-1)\delta(k) > 0 \\ -\varphi_\alpha \alpha(k) & \text{if } \bar{\delta}(k-1)\delta(k) < 0 \\ 0 & \text{otherwise} \end{cases} \tag{7}$$

where $\kappa_\alpha$ is the constant learning coefficient scale factor, exp is the exponential function, $\varphi_\alpha$ is the constant learning coefficient decrement factor, and $\gamma_\alpha$ is the constant learning coefficient exponential factor. The momentum coefficient change is also written as

$$\Delta\mu(k) = \begin{cases} \kappa_\mu \exp(-\gamma_\mu \left|\bar{\delta}(k)\right|) & \text{if } \bar{\delta}(k-1)\delta(k) > 0 \\ -\varphi_\mu \mu(k) & \text{if } \bar{\delta}(k-1)\delta(k) < 0 \\ 0 & \text{otherwise} \end{cases} \tag{8}$$

where $\kappa_\mu$ is the constant momentum coefficient scale factor, $\varphi_\mu$ is the constant momentum coefficient decrement factor, and $\gamma_\mu$ is the constant momentum coefficient exponential factor. In order to take a step further to prevent wild jumps and oscillations in the weight space, ceilings are placed on the individual connection learning and momentum coefficients [23].

2.1.4. *Directed random search (DRS) algorithm.* The directed random search is a reinforcement learning approach and used to calculate the weights of ANNs. This algorithm also tries to minimize the overall error [24]. Random steps are taken in the weights and a directed component is added to the random step to enable an impetus to pursue previously search directions. The DRS is based on four procedures as random step, reversal step, directed procedure and self-tuning variance. In the random step, a random value is added to each weight of network and the error is then evaluated for all training sets as

$$w(k+1) = w_{best} + dw(k) \tag{9}$$

where $w_{best}$ is the best weight vector previous to iteration $k$ and $dw(k)$ is the delta weight vector at iteration $k$. Depending on the error evaluation, the weights are replaced with the new weights. If there is no improvement at the error in the random step, some random value is subtracted from the weight value during the reversal step, that is

$$w(k+1) = w_{best} - dw(k) \tag{10}$$

In [24], a directed procedure has been added to the random step to further improve with reversals. The new weights are obtained from:

$$w(k+1) = w_{best} - dw(k) + dp(k) \tag{11}$$

where $dp(k)$ is the directed procedure and based on the history of success or failure of the random steps.

2.1.5. *Quick propagation (QP) algorithm.* The QP algorithm was developed by Fahlman [25] as a new method of improving the rate of convergence in MLPs. First, the changes in weights are calculated as

$$\Delta w(k) = \varepsilon L(k) + \alpha Q(k) \tag{12}$$

where $\varepsilon$ and $\alpha$ are the learning coefficients for the linear and the quadratic terms, respectively,

$$L(k) = \begin{cases} h(k) & \text{if } h(k)h(k-1) \geq 0 \\ 0 & \text{otherwise} \end{cases} \tag{13}$$

and

$$Q(k) = \begin{cases} \mu \Delta w(k-1) & \text{if } h(k)\left(h(k) - \left(\frac{\mu}{\mu+1}\right) h(k-1)\right) \geq 0 \\ \Delta q(k) & \text{otherwise} \end{cases} \tag{14}$$

In Equations (13) and (14), the variables are shown as follows: $h(k) = \partial E/\partial w(k)$ is the gradient calculated by the BP, accumulated from epoch $k-1$ to epoch $k$, and normalized with respect to epoch size and number of weights incoming to the neuron, $\Delta w(k)$ is the change in weight from epoch $k-1$ to epoch $k$ ignoring weight decay and clipping, $\mu$ is the maximum growth factor, and $\Delta q(k) = (\Delta w(k)h(k))/(h(k-1) - h(k))$ is the step that jumps to minimum of parabola. The weight is then updated using the delta weight and the weight decay coefficient:

$$w(k) = (1-\delta)w(k-1) + \Delta w(k) \tag{15}$$

where $\delta$ is the decay rate.

2.2. **Radial basis function neural network (RBFNN).** An alternative network architecture to the MLP is the RBFN. Figure 2 shows the structure of the RBF neural network, which comprises of three layers. The hidden layer possesses an array of neurons, referred to as the computing units. The number of such units can be varied depending on user's requirement [18,26]. Different basis functions like spline, multi-quadratic, and Gaussian functions have been studied, but the most widely used one is the Gaussian type.

In comparison to the other types of neural network used for pattern classification like back propagation feedforward networks, the RBF network requires less computation time for learning and has a more compact topology. The Gaussian RBF is found not only

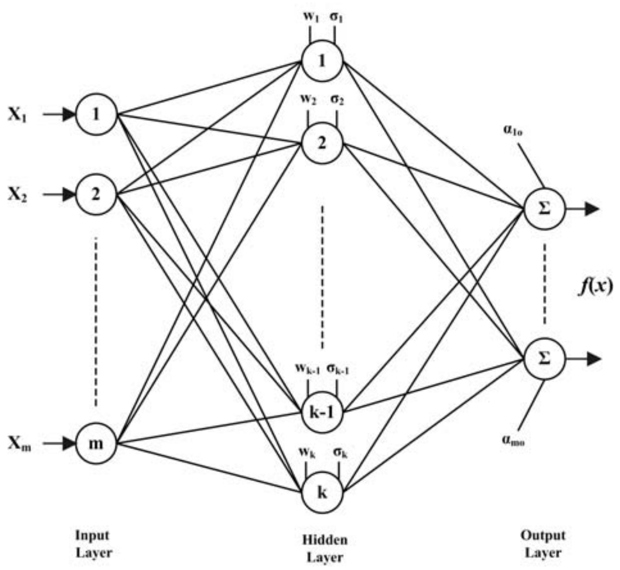


Figure 2. The structure of RBF neural network

suitable in generalizing a global mapping but also in refining local features without altering the already learned mapping. Each hidden unit in the network has two parameters called a center ($\omega$) and a width ($\sigma$) associated with it. The response of one such hidden unit to the network input $\boldsymbol{X}$, $\boldsymbol{X} = [x_1, x_2, \ldots, x_n]^T$ is expressed as:

$$\phi_k(\boldsymbol{X}) = \exp\left(-\frac{1}{\sigma_k^2}\left\|\boldsymbol{X} - \omega_k\right\|^2\right) \tag{16}$$

where $\omega_k$ is the center vector for $k$th hidden unit, $\sigma_k$ is the width of the Gaussian function, and $\|\ \|$ denotes the Euclidean norm. The output layer comprises a number of nodes depending on the number of fault types to be classified which perform simple summation. The response of each hidden unit (1) is scaled by its connecting weights ($\alpha$'s) to the output nodes and then summed to produce the overall network output. The overall network output is expressed as:

$$f_m(\boldsymbol{X}) = \alpha_{mo} + \sum_{k=1}^{N} \alpha_{mk}\phi_k(\boldsymbol{X}) \tag{17}$$

where $N$ indicates the total number of hidden neurons in the network, $\alpha_{mk}$ is the connecting weight of the $k$th hidden unit to $m$th output node, and $\alpha_{mo}$ is the bias term for the corresponding $m$th output neuron. The learning process of the RBFNN involves with the allocation of new hidden units and tuning of network parameters. The learning process is terminated when the output error goes under the defined threshold [27].

3. **Training Artificial Neural Network.** The sample system considered for explanation of the proposed methodology and training ANNs is a network shown in Figure 3. In [15,16], an ANN is trained to evaluate overvoltages; but it is necessary to train an ANN for every system. In this paper, training of ANN is performed based on equivalent circuits of Figure 3. In other words, the equivalent parameters of the network are added to ANN inputs to achieve good generalization capability for developed ANNs. In fact, in this approach ANN is trained just once for sample system of Figure 3. It is just sufficient to convert every studied system to equivalent system of Figure 3; then it is possible to use developed ANNs to evaluate overvoltages. Therefore, developed ANNs can be applied to every studied system.

To train ANNs, all experiments have been repeated for different system parameters. After learning, all parameters of the trained networks have been frozen and then used in the retrieval mode for testing the capabilities of the system on the data not used in learning. The testing data samples have been generated through the PSB program by placing the parameter values not used in learning, by applying different parameters. A large number of testing data have been used to check the proposed solution in the most objective way at practically all possible parameters variation. Relative error is calculated by the difference of PSB output and ANN output:

$$\mathrm{Er}_{\mathrm{Relative}}(\%) = \frac{|\mathrm{ANN} - \mathrm{PSB}|}{\mathrm{PSB}} \times 100 \tag{18}$$

and absolute error is calculated as:

$$\mathrm{Er}_{\mathrm{Absolute}} = |\mathrm{ANN} - \mathrm{PSB}| \tag{19}$$

Specification of ANNs is presented in Table 1.

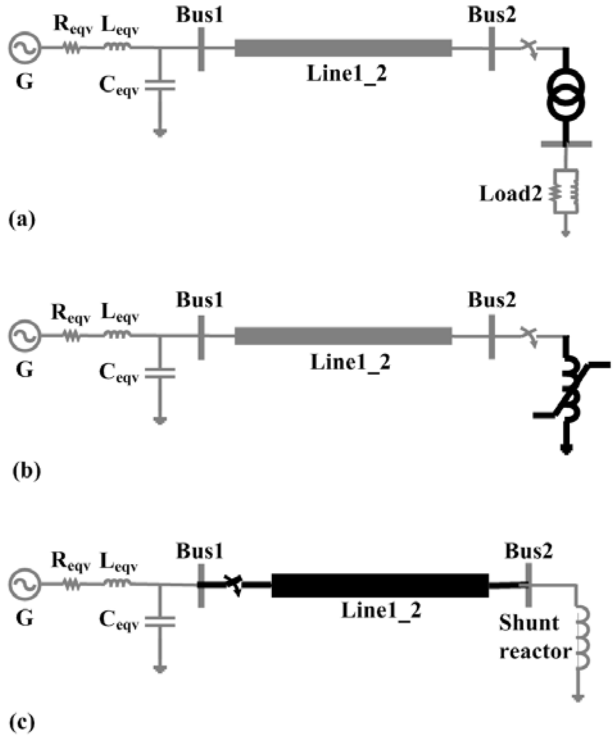


Figure 3. Sample systems for power equipment energization study. (a) Transformer energization, (b) shunt reactor energization, and (c) transmission line energization. G: generator, $R_{eqv}$: equivalent resistance, $L_{eqv}$: equivalent inductance, and $C_{eqv}$: equivalent capacitance.

Table 1. Specification of developed ANNs

| **ANN model** | **Number of hidden layers** | **Number of neurons in each hidden layer** | **Training time [epochs]** |
|---|---|---|---|
| BP | 2 | 10 | 50 |
| DBD | 3 | 6 | 165 |
| EDBD | 3 | 7 | 69 |
| DRS | 3 | 6 | 43 |
| QP | 3 | 5 | 146 |
| RBF | 2 | 10 | 85 |

3.1. **Transformer switching study.** The major cause of harmonic resonance overvoltage problems is the switching of lightly loaded transformers at the end of transmission lines. The harmonic-current components of the same frequency as the system resonance frequencies are amplified in case of parallel resonance, thereby creating higher voltages at the transformer terminals. This leads to a higher level of saturation, resulting in higher harmonic components of the inrush current that again results in increased voltages. This can happen particularly in lightly damped systems, common at the beginning of a restoration procedure when a path from a black-start source to a large power plant is being established and only a few loads are restored yet [1,8]. Overvoltage will put the transformer into saturation, causing core heating and copious harmonic current generation. Circuit breaker called upon to operate during periods of high voltage will reduce interrupting capability.

Unlike [16], which is applicable for single-phase transformers and its evaluation is based on RBF, this work proposed an approach for three-phase systems and its evaluation is based on six ANN models. Also, equivalent circuit parameters are selected as ANN inputs to enhance generalization capability of the developed ANN. Moreover, in [16] operators need to determine switching angle and remanent flux which is very difficult; whereas as mentioned below, there is no need to these parameters.

Normally for harmonic overvoltages analysis during transformer energization, the worst case of the switching angle and remanent flux must be considered which is a function of switching time, transformer characteristics and its initial flux condition, and impedance characteristics of the switching bus [28]. Using the worst switching angle and remanent flux, the number of simulations for each case can be reduced significantly.

In order to determine worst-case switching time and remanent flux, the following index is defined as

$$W = \sum_{h=2}^{10} Z_{jj}(h) \cdot I_j(h, t_0, \phi_r) \tag{20}$$

where $t_0$ is the switching time, $\phi_r$ is the initial transformer flux, and $h$ is the harmonic number. This index can be a definition for the worst-case switching condition and remanent flux. Using a numerical algorithm, one can find the switching time and remanent flux for which $W$ is maximal (i.e., harmonic overvoltage is maximal).

Figure 4(a) shows the result of the PSB frequency analysis at bus 2 (Figure 3(a)). The magnitude of the thevenin impedance, seen from bus 2, $Z_{\mathrm{bus2}}$ shows a parallel resonance peak at 246 Hz. Figures 4(b), 4(c) and 4(d) show changes of $W$ index with respect to the current starting angle and remanent flux for three phases. As shown in Figure 4, $W_{\mathrm{max,B}}$ is bigger than $W_{\mathrm{max,A}}$ and $W_{\mathrm{max,C}}$. Therefore, if simulation is performed based on switching angle and remanent flux related to $W_{\mathrm{max,B}}$, maximum overvoltages is achieved. Table 2 summarizes the results of overvoltages simulation for four different switching angles and remanent fluxes including $W_{\mathrm{max,A}}$ (80° and 0.62 p.u.), $W_{\mathrm{max,B}}$ (39° and 0.65 p.u.), $W_{\mathrm{max,C}}$ (87° and 0.09 p.u.). Results verify the effectiveness of $W$ index.

Based on this approach, switching angle and remanent flux are eliminated from ANN inputs; thus, ANN training procedure time is reduced significantly. Therefore, for training ANN, following parameters are considered as ANN inputs:

- Voltage at transformer bus before switching
- Equivalent resistance of the network
- Equivalent inductance of the network
- Equivalent capacitance of the network
- Line length
- Saturation curve slope

The steps for harmonic overvoltages assessment and estimation are listed below:

1) Determine the characteristics of transformer that should be energized.
2) Calculate the $Z_{ii}(h)$ at the transformer bus for $h = 2f_0, \ldots, 10f_0$.
3) Compute the worst switching angle and remanent flux for simulation.
4) Run PSB simulation.
5) Determine the overvoltage peak and duration.
6) Repeat Steps 1 to 5 with various system parameters to learn artificial neural network.
7) Test the artificial neural network with different system parameters.

Schematic diagram of transformer energization study during power system restoration is illustrated in Figure 5.

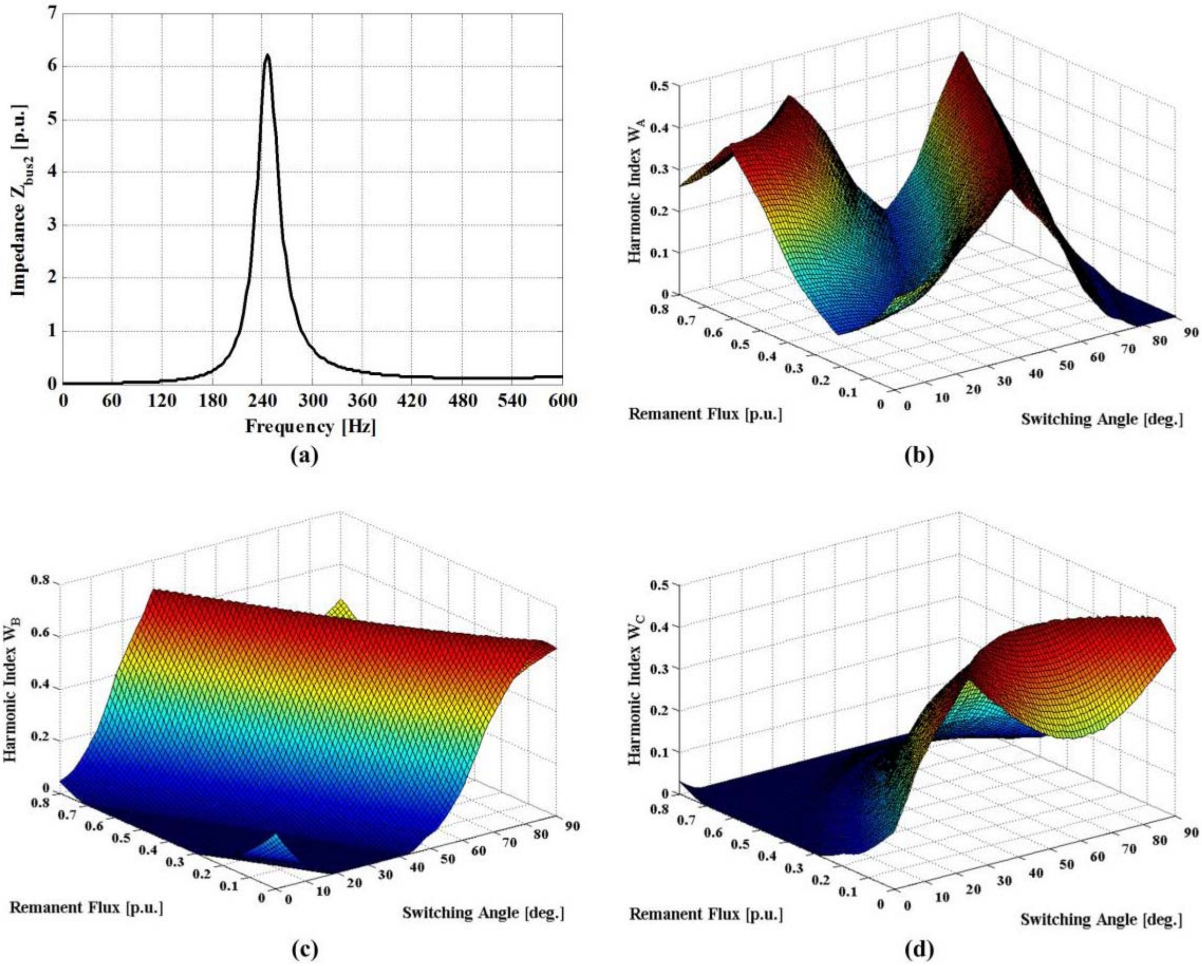


FIGURE 4. (a) Impedance at bus 2 of Figure 2(a), and changes of $W$ index with respect to current starting angle and remanent flux in (b) Phase A, (c) Phase B, and (d) Phase C.

TABLE 2. Effect of switching time and remanent flux on the maximum of overvoltages and duration of $V_{peak} > 1.3$ p.u.

| **Transformer Energization Study:** | | | |
|---|---|---|---|
| **Switching Angle [deg.]** | **Remanent Flux [p.u.]** | **$V_{peak}$ [p.u.]** | **Duration of ($V_{peak} > 1.3$ p.u.) [s]** |
| 39 | 0.65 | 2.1961 | 0.7544 |
| 80 | 0.62 | 1.8095 | 0.4627 |
| 87 | 0.09 | 1.8831 | 0.8469 |
| 15 | 0.3 | 1.5319 | 0.2753 |
| **Shunt Reactor Energization Study:** | | | |
| **Switching Angle [deg.]** | **Remanent Flux [p.u.]** | **$V_{peak}$ [p.u.]** | **Duration of ($V_{peak} > 1.3$ p.u.) [s]** |
| 20 | 0.27 | 1.9205 | 0.5628 |
| 20 | 0.65 | 1.5841 | 0.3394 |
| 75 | 0.27 | 1.6537 | 0.3064 |
| 60 | 0.5 | 1.5293 | 0.2675 |

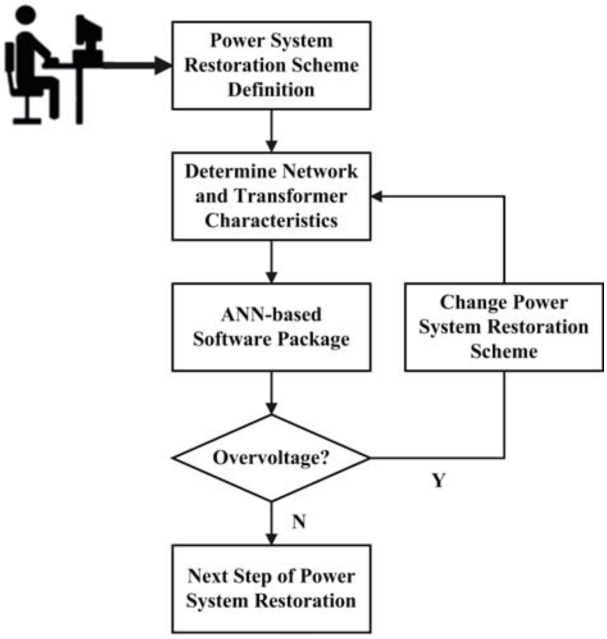


FIGURE 5. ANN-based approach to analyze switching overvoltages during transformer energization

3.2. **Shunt reactor energization study.** Long EHV transmission lines are generally compensated by means of shunt reactor sets. Reactor failures have directed attention to the transient overvoltages generated by reactor switching. Shunt reactors are applied to regulate the reactive power balance of a system by means of compensating for the surplus reactive power generation of transmission lines. Reactors are normally disconnected at heavy load and connected to the lines at periods of low load. Consequently, frequent switching is a significant characteristic of shunt reactors in order that they can react to the changing system load condition [29].

Transients caused by shunt reactor switching have been an important parameter in the design of the relevant equipment (reactor, circuit breaker, insulation) of power systems. Based on considered model for shunt reactor, it is possible to use harmonic index which is defined in previous section. Table 2 summarizes the results of overvoltages simulation for four different switching angles and remanent fluxes that verify the effectiveness of $W$ index for shunt reactor energization study.

Consequently, in this case following parameters are selected as ANN inputs:

- Voltage at shunt reactor bus before switching
- Equivalent resistance of the network
- Equivalent inductance of the network
- Equivalent capacitance of the network
- Line length
- Shunt reactor capacity
- Saturation curve slope

The steps of overvoltages assessment and estimation follow:

1) Determine the characteristics of shunt reactor that should be energized.
2) Calculate the $Z_{ii}(h)$ at the shunt reactor bus for $h = 2f_0, \ldots, 10f_0$.
3) Compute the worst switching angle and remanent flux for simulation.
4) Run PSB simulation.
5) Determine the overvoltage peak and duration.

Table 3. Some sample testing data and output for transformer energization

| **Backpropagation:** | | | | | | | |
|---|---|---|---|---|---|---|---|
| **V** | **L.L.** | **$V_{PSB}$** | **$V_{BP}$** | **$error_V$** | **$T_{PSB}$** | **$T_{BP}$** | **$error_T$** |
| 0.9212 | 146 | 1.3018 | 1.2695 | 2.4828 | 0.0826 | 0.0839 | 1.5142 |
| 0.9405 | 175 | 1.3477 | 1.3121 | 2.6414 | 0.2148 | 0.2197 | 2.2942 |
| 0.9822 | 205 | 1.4961 | 1.4816 | 0.9661 | 0.3561 | 0.3547 | 0.3841 |
| 0.1006 | 227 | 1.5908 | 1.6286 | 2.3790 | 0.4459 | 0.4313 | 3.2682 |
| 1.0629 | 240 | 1.7606 | 1.8010 | 2.2928 | 0.4103 | 0.4076 | 0.6561 |
| 1.0891 | 265 | 1.8247 | 1.8351 | 0.5691 | 0.5719 | 0.5666 | 0.9316 |
| 1.1714 | 290 | 1.9072 | 1.9151 | 0.4165 | 0.5246 | 0.5100 | 2.7924 |
| 1.2073 | 316 | 1.9208 | 1.8873 | 1.7443 | 0.6128 | 0.6233 | 1.7066 |
| **Delta-bar-delta:** | | | | | | | |
| **V** | **L.L.** | **$V_{PSB}$** | **$V_{DBD}$** | **$error_V$** | **$T_{PSB}$** | **$T_{DBD}$** | **$error_T$** |
| 0.9212 | 146 | 1.3018 | 1.2647 | 2.8515 | 0.0826 | 0.0799 | 3.2491 |
| 0.9405 | 175 | 1.3477 | 1.3050 | 3.1703 | 0.2148 | 0.2104 | 2.0303 |
| 0.9822 | 205 | 1.4961 | 1.5027 | 0.4445 | 0.3561 | 0.3559 | 0.0594 |
| 0.1006 | 227 | 1.5908 | 1.6417 | 3.1968 | 0.4459 | 0.4440 | 0.4230 |
| 1.0629 | 240 | 1.7606 | 1.7216 | 2.2133 | 0.4103 | 0.4227 | 3.0195 |
| 1.0891 | 265 | 1.8247 | 1.8309 | 0.3414 | 0.5719 | 0.5816 | 1.6950 |
| 1.1714 | 290 | 1.9072 | 1.9258 | 0.9747 | 0.5246 | 0.5091 | 2.9570 |
| 1.2073 | 316 | 1.9208 | 1.8840 | 1.9141 | 0.6128 | 0.6083 | 0.7329 |
| **Extended delta-bar-delta:** | | | | | | | |
| **V** | **L.L.** | **$V_{PSB}$** | **$V_{EDBD}$** | **$error_V$** | **$T_{PSB}$** | **$T_{EDBD}$** | **$error_T$** |
| 0.9212 | 146 | 1.3018 | 1.3277 | 1.9909 | 0.0826 | 0.0849 | 2.7368 |
| 0.9405 | 175 | 1.3477 | 1.3698 | 1.6429 | 0.2148 | 0.2156 | 0.3521 |
| 0.9822 | 205 | 1.4961 | 1.4955 | 0.0417 | 0.3561 | 0.3524 | 1.0292 |
| 0.1006 | 227 | 1.5908 | 1.5720 | 1.1799 | 0.4459 | 0.4496 | 0.8308 |
| 1.0629 | 240 | 1.7606 | 1.7506 | 0.5676 | 0.4103 | 0.4179 | 1.8581 |
| 1.0891 | 265 | 1.8247 | 1.7740 | 2.7800 | 0.5719 | 0.5701 | 0.3202 |
| 1.1714 | 290 | 1.9072 | 1.9280 | 1.0893 | 0.5246 | 0.5320 | 1.4186 |
| 1.2073 | 316 | 1.9208 | 1.8853 | 1.8499 | 0.6128 | 0.6150 | 0.3670 |
| **Directed random search:** | | | | | | | |
| **V** | **L.L.** | **$V_{PSB}$** | **$V_{DRS}$** | **$error_V$** | **$T_{PSB}$** | **$T_{DRS}$** | **$error_T$** |
| 0.9212 | 146 | 1.3018 | 1.2620 | 3.0561 | 0.0826 | 0.0851 | 2.9775 |
| 0.9405 | 175 | 1.3477 | 1.3237 | 1.7798 | 0.2148 | 0.2190 | 1.9620 |
| 0.9822 | 205 | 1.4961 | 1.4714 | 1.6535 | 0.3561 | 0.3677 | 3.2536 |
| 0.1006 | 227 | 1.5908 | 1.6615 | 4.4459 | 0.4459 | 0.4350 | 2.4383 |
| 1.0629 | 240 | 1.7606 | 1.7576 | 0.1698 | 0.4103 | 0.4187 | 2.0398 |
| 1.0891 | 265 | 1.8247 | 1.7520 | 3.9833 | 0.5719 | 0.5882 | 2.8539 |
| 1.1714 | 290 | 1.9072 | 1.9856 | 4.1098 | 0.5246 | 0.5085 | 3.0765 |
| 1.2073 | 316 | 1.9208 | 1.8520 | 3.5828 | 0.6128 | 0.6340 | 3.4612 |
| **Quick propagation:** | | | | | | | |
| **V** | **L.L.** | **$V_{PSB}$** | **$V_{QP}$** | **$error_V$** | **$T_{PSB}$** | **$T_{QP}$** | **$error_T$** |
| 0.9212 | 146 | 1.3018 | 1.3144 | 0.9692 | 0.0826 | 0.0830 | 0.5027 |
| 0.9405 | 175 | 1.3477 | 1.3499 | 0.1616 | 0.2148 | 0.2161 | 0.6133 |
| 0.9822 | 205 | 1.4961 | 1.5012 | 0.3400 | 0.3561 | 0.3452 | 3.0539 |
| 0.1006 | 227 | 1.5908 | 1.6366 | 2.8821 | 0.4459 | 0.4558 | 2.2283 |
| 1.0629 | 240 | 1.7606 | 1.8034 | 2.4319 | 0.4103 | 0.4068 | 0.8537 |
| 1.0891 | 265 | 1.8247 | 1.8044 | 1.1098 | 0.5719 | 0.5846 | 2.2275 |
| 1.1714 | 290 | 1.9072 | 1.8438 | 3.3258 | 0.5246 | 0.5211 | 0.6642 |
| 1.2073 | 316 | 1.9208 | 1.9185 | 0.1206 | 0.6128 | 0.6143 | 0.2474 |
| **Radial basis function:** | | | | | | | |
| **V** | **L.L.** | **$V_{PSB}$** | **$V_{RBF}$** | **$error_V$** | **$T_{PSB}$** | **$T_{RBF}$** | **$error_T$** |
| 0.9212 | 146 | 1.3018 | 1.3454 | 3.3513 | 0.0826 | 0.0812 | 1.7433 |
| 0.9405 | 175 | 1.3477 | 1.3932 | 3.3771 | 0.2148 | 0.2216 | 3.1530 |
| 0.9822 | 205 | 1.4961 | 1.4878 | 0.5516 | 0.3561 | 0.3489 | 2.0113 |
| 0.1006 | 227 | 1.5908 | 1.6448 | 3.3971 | 0.4459 | 0.4327 | 2.9581 |
| 1.0629 | 240 | 1.7606 | 1.7016 | 3.3501 | 0.4103 | 0.4209 | 2.5852 |
| 1.0891 | 265 | 1.8247 | 1.8557 | 1.6988 | 0.5719 | 0.5836 | 2.0510 |
| 1.1714 | 290 | 1.9072 | 1.8538 | 2.8010 | 0.5246 | 0.5201 | 0.8636 |
| 1.2073 | 316 | 1.9208 | 1.9303 | 0.4966 | 0.6128 | 0.6271 | 2.3325 |

V = voltage at transformer bus before switching [p.u.], L.L. = line length [km], $V_{PSB}$ = overvoltage peak calculated by PSB [p.u.], $V_{BP}$= overvoltage peak calculated by BP [p.u.], $V_{DBD}$ = overvoltage peak calculated by BDB [p.u.], $V_{EDBD}$ = overvoltage peak calculated by EBDB [p.u.], $V_{DRS}$ = overvoltage peak calculated by DRS [p.u.], $V_{QP}$ = overvoltage peak calculated by QP [p.u.], $V_{RBF}$ = overvoltage peak calculated by RBF [p.u.], $T_{PSB}$ = overvoltage duration calculated by PSB [s], $T_{BP}$ = overvoltage duration calculated by BP [s], $T_{DBD}$ = overvoltage duration calculated by BDB [s], $T_{EDBD}$ = overvoltage duration calculated by EBDB [s], $T_{DRS}$ = overvoltage duration calculated by DRS [s], $T_{QP}$ = overvoltage duration calculated by QP [s], $T_{RBF}$ = overvoltage duration calculated by RBF [s], $error_V$ = voltage error [%], $error_T$ = duration time error [%], Phase = phases that have maximum overvoltages.

TABLE 4. Some sample testing data and output for shunt reactor energization

| **Backpropagation:** | | | | | | | | |
|---|---|---|---|---|---|---|---|---|
| **V** | **L.L.** | **S.R.** | $V_{PSB}$ | $V_{BP}$ | $error_V$ | $T_{PSB}$ | $T_{BP}$ | $error_T$ |
| 1.1442 | 150 | 70 | 1.5011 | 1.4944 | 0.4442 | 0.1936 | 0.1925 | 0.5640 |
| 1.1561 | 165 | 45 | 1.5453 | 1.5271 | 1.1784 | 0.2375 | 0.2438 | 2.6534 |
| 1.2302 | 178 | 30 | 1.6769 | 1.6516 | 1.5091 | 0.3469 | 0.3363 | 3.0489 |
| 1.2514 | 200 | 30 | 1.7481 | 1.8016 | 3.0588 | 0.3952 | 0.4001 | 1.2277 |
| 1.3326 | 215 | 23 | 1.9507 | 1.9387 | 0.6145 | 0.5104 | 0.5226 | 2.3994 |
| 1.3326 | 215 | 17 | 1.9914 | 1.9268 | 3.2455 | 0.5536 | 0.5593 | 1.0295 |
| 1.4165 | 230 | 17 | 2.1652 | 2.1548 | 0.4804 | 0.6742 | 0.6867 | 1.8572 |
| 1.4327 | 242 | 10 | 2.2479 | 2.3140 | 2.9419 | 0.7593 | 0.7372 | 2.9135 |
| **Delta-bar-delta:** | | | | | | | | |
| **V** | **L.L.** | **S.R.** | $V_{PSB}$ | $V_{DBD}$ | $error_V$ | $T_{PSB}$ | $T_{DBD}$ | $error_T$ |
| 1.1442 | 150 | 70 | 1.5011 | 1.5092 | 0.5378 | 0.1936 | 0.1999 | 3.2751 |
| 1.1561 | 165 | 45 | 1.5453 | 1.5605 | 0.9835 | 0.2375 | 0.2337 | 1.6026 |
| 1.2302 | 178 | 30 | 1.6769 | 1.7027 | 1.5403 | 0.3469 | 0.3498 | 0.8417 |
| 1.2514 | 200 | 30 | 1.7481 | 1.7158 | 1.8450 | 0.3952 | 0.3846 | 2.6736 |
| 1.3326 | 215 | 23 | 1.9507 | 1.9195 | 1.6010 | 0.5104 | 0.4968 | 2.6576 |
| 1.3326 | 215 | 17 | 1.9914 | 2.0524 | 3.0638 | 0.5536 | 0.5680 | 2.5923 |
| 1.4165 | 230 | 17 | 2.1652 | 2.1259 | 1.8132 | 0.6742 | 0.6917 | 2.6029 |
| 1.4327 | 242 | 10 | 2.2479 | 2.1737 | 3.3027 | 0.7593 | 0.7565 | 0.3707 |
| **Extended delta-bar-delta:** | | | | | | | | |
| **V** | **L.L.** | **S.R.** | $V_{PSB}$ | $V_{EDBD}$ | $error_V$ | $T_{PSB}$ | $T_{EDBD}$ | $error_T$ |
| 1.1442 | 150 | 70 | 1.5011 | 1.5441 | 2.8622 | 0.1936 | 0.1988 | 2.6914 |
| 1.1561 | 165 | 45 | 1.5453 | 1.5312 | 0.9125 | 0.2375 | 0.2342 | 1.3860 |
| 1.2302 | 178 | 30 | 1.6769 | 1.7118 | 2.0802 | 0.3469 | 0.3502 | 0.9553 |
| 1.2514 | 200 | 30 | 1.7481 | 1.7495 | 0.0788 | 0.3952 | 0.3957 | 0.1303 |
| 1.3326 | 215 | 23 | 1.9507 | 1.9217 | 1.4884 | 0.5104 | 0.5224 | 2.3565 |
| 1.3326 | 215 | 17 | 1.9914 | 1.9696 | 1.0945 | 0.5536 | 0.5619 | 1.5035 |
| 1.4165 | 230 | 17 | 2.1652 | 2.1530 | 0.5652 | 0.6742 | 0.6849 | 1.5811 |
| 1.4327 | 242 | 10 | 2.2479 | 2.2338 | 0.6257 | 0.7593 | 0.7431 | 2.1345 |
| **Directed random search:** | | | | | | | | |
| **V** | **L.L.** | **S.R.** | $V_{PSB}$ | $V_{DRS}$ | $error_V$ | $T_{PSB}$ | $T_{DRS}$ | $error_T$ |
| 1.1442 | 150 | 70 | 1.5011 | 1.5568 | 3.7097 | 0.1936 | 0.1878 | 3.0204 |
| 1.1561 | 165 | 45 | 1.5453 | 1.4770 | 4.4220 | 0.2375 | 0.2299 | 3.2185 |
| 1.2302 | 178 | 30 | 1.6769 | 1.7320 | 3.2861 | 0.3469 | 0.3369 | 2.8893 |
| 1.2514 | 200 | 30 | 1.7481 | 1.7752 | 1.5474 | 0.3952 | 0.3877 | 1.8857 |
| 1.3326 | 215 | 23 | 1.9507 | 1.8994 | 2.6283 | 0.5104 | 0.5014 | 1.7584 |
| 1.3326 | 215 | 17 | 1.9914 | 1.9817 | 0.4850 | 0.5536 | 0.5333 | 3.6726 |
| 1.4165 | 230 | 17 | 2.1652 | 2.2535 | 4.0784 | 0.6742 | 0.6838 | 1.4284 |
| 1.4327 | 242 | 10 | 2.2479 | 2.3369 | 3.9584 | 0.7593 | 0.7871 | 3.6654 |
| **Quick propagation:** | | | | | | | | |
| **V** | **L.L.** | **S.R.** | $V_{PSB}$ | $V_{QP}$ | $error_V$ | $T_{PSB}$ | $T_{QP}$ | $error_T$ |
| 1.1442 | 150 | 70 | 1.5011 | 1.5525 | 3.4254 | 0.1936 | 0.1997 | 3.1252 |
| 1.1561 | 165 | 45 | 1.5453 | 1.5068 | 2.4944 | 0.2375 | 0.2433 | 2.4613 |
| 1.2302 | 178 | 30 | 1.6769 | 1.7063 | 1.7517 | 0.3469 | 0.3536 | 1.9451 |
| 1.2514 | 200 | 30 | 1.7481 | 1.7769 | 1.6488 | 0.3952 | 0.3926 | 0.6455 |
| 1.3326 | 215 | 23 | 1.9507 | 1.9466 | 0.2087 | 0.5104 | 0.5142 | 0.7421 |
| 1.3326 | 215 | 17 | 1.9914 | 2.0389 | 2.3869 | 0.5536 | 0.5521 | 0.2707 |
| 1.4165 | 230 | 17 | 2.1652 | 2.1620 | 0.1485 | 0.6742 | 0.6958 | 3.1983 |
| 1.4327 | 242 | 10 | 2.2479 | 2.2423 | 0.2501 | 0.7593 | 0.7405 | 2.4735 |
| **Radial basis function:** | | | | | | | | |
| **V** | **L.L.** | **S.R.** | $V_{PSB}$ | $V_{RBF}$ | $error_V$ | $T_{PSB}$ | $T_{RBF}$ | $error_T$ |
| 1.1442 | 150 | 70 | 1.5011 | 1.4751 | 1.7296 | 0.1936 | 0.2014 | 4.0248 |
| 1.1561 | 165 | 45 | 1.5453 | 1.5032 | 2.7267 | 0.2375 | 0.2430 | 2.3245 |
| 1.2302 | 178 | 30 | 1.6769 | 1.6349 | 2.5026 | 0.3469 | 0.3579 | 3.1622 |
| 1.2514 | 200 | 30 | 1.7481 | 1.6928 | 3.1630 | 0.3952 | 0.3979 | 0.6912 |
| 1.3326 | 215 | 23 | 1.9507 | 1.8899 | 3.1182 | 0.5104 | 0.4885 | 4.2906 |
| 1.3326 | 215 | 17 | 1.9914 | 1.9681 | 1.1696 | 0.5536 | 0.5401 | 2.4340 |
| 1.4165 | 230 | 17 | 2.1652 | 2.2182 | 2.4456 | 0.6742 | 0.6536 | 3.0588 |
| 1.4327 | 242 | 10 | 2.2479 | 2.2323 | 0.6923 | 0.7593 | 0.7605 | 0.1645 |

V = voltage at reactor bus before switching [p.u.], L.L. = line length [km], S.R. = shunt reactor capacity [MVAR], $V_{PSB}$ = overvoltage peak calculated by PSB [p.u.], $V_{BP}$ = overvoltage peak calculated by BP [p.u.], $V_{DBD}$ = overvoltage peak calculated by BDB [p.u.], $V_{EDBD}$ = overvoltage peak calculated by EBDB [p.u.], $V_{DRS}$ = overvoltage peak calculated by DRS [p.u.], $V_{QP}$ = overvoltage peak calculated by QP [p.u.], $V_{RBF}$ = overvoltage peak calculated by RBF [p.u.], $T_{PSB}$ = overvoltage duration calculated by PSB [s], $T_{BP}$ = overvoltage duration calculated by BP [s], $T_{DBD}$ = overvoltage duration calculated by BDB [s], $T_{EDBD}$ = overvoltage duration calculated by EBDB [s], $T_{DRS}$ = overvoltage duration calculated by DRS [s], $T_{QP}$ = overvoltage duration calculated by QP [s], $T_{RBF}$ = overvoltage duration calculated by RBF [s], $error_V$ = voltage error [%], $error_T$ = duration time error [%], Phase = phases that have maximum overvoltages.

TABLE 5. Some sample testing data and output for transmission line energization

**Backpropagation:**

| V | S.A. | L.L. | S.R. | $V_{PSB}$ | $V_{BP}$ | $error_V$ | $T_{PSB}$ | $T_{BP}$ | $error_T$ |
|---|---|---|---|---|---|---|---|---|---|
| 0.9491 | 30 | 375 | 40 | 2.3508 | 2.3666 | 0.6721 | 0.3652 | 0.3759 | 2.9233 |
| 0.9127 | 30 | 240 | 40 | 2.2769 | 2.2880 | 0.4861 | 0.3107 | 0.3142 | 1.1286 |
| 0.9973 | 60 | 240 | 55 | 2.3016 | 2.2455 | 2.4369 | 0.3496 | 0.3428 | 1.9329 |
| 0.9754 | 75 | 195 | 12 | 2.3882 | 2.3960 | 0.3284 | 0.4073 | 0.4213 | 3.4270 |
| 1.0719 | 15 | 315 | 23 | 2.4195 | 2.4640 | 1.8389 | 0.4217 | 0.4136 | 1.9226 |
| 1.0592 | 5 | 282 | 45 | 2.3725 | 2.4165 | 1.8562 | 0.3846 | 0.3802 | 1.1565 |
| 1.0946 | 45 | 137 | 63 | 2.3596 | 2.2885 | 3.0140 | 0.3378 | 0.3305 | 2.1682 |
| 1.1123 | 53 | 346 | 10 | 2.8537 | 2.9021 | 1.6970 | 0.5449 | 0.5518 | 1.2622 |

**Delta-bar-delta:**

| V | S.A. | L.L. | S.R. | $V_{PSB}$ | $V_{DBD}$ | $error_V$ | $T_{PSB}$ | $T_{DBD}$ | $error_T$ |
|---|---|---|---|---|---|---|---|---|---|
| 0.9491 | 30 | 375 | 40 | 2.3508 | 2.3013 | 2.1076 | 0.3652 | 0.3608 | 1.2015 |
| 0.9127 | 30 | 240 | 40 | 2.2769 | 2.2461 | 1.3537 | 0.3107 | 0.3005 | 3.2761 |
| 0.9973 | 60 | 240 | 55 | 2.3016 | 2.2278 | 3.2060 | 0.3496 | 0.3481 | 0.4367 |
| 0.9754 | 75 | 195 | 12 | 2.3882 | 2.3883 | 0.0040 | 0.4073 | 0.3969 | 2.5570 |
| 1.0719 | 15 | 315 | 23 | 2.4195 | 2.3803 | 1.6186 | 0.4217 | 0.4122 | 2.2627 |
| 1.0592 | 5 | 282 | 45 | 2.3725 | 2.3373 | 1.4852 | 0.3846 | 0.3958 | 2.9160 |
| 1.0946 | 45 | 137 | 63 | 2.3596 | 2.3977 | 1.6132 | 0.3378 | 0.3331 | 1.3940 |
| 1.1123 | 53 | 346 | 10 | 2.8537 | 2.7768 | 2.6956 | 0.5449 | 0.5592 | 2.6244 |

**Extended delta-bar-delta:**

| V | S.A. | L.L. | S.R. | $V_{PSB}$ | $V_{EDBD}$ | $error_V$ | $T_{PSB}$ | $T_{EDBD}$ | $error_T$ |
|---|---|---|---|---|---|---|---|---|---|
| 0.9491 | 30 | 375 | 40 | 2.3508 | 2.3061 | 1.9036 | 0.3652 | 0.3581 | 1.9505 |
| 0.9127 | 30 | 240 | 40 | 2.2769 | 2.2194 | 2.5237 | 0.3107 | 0.3191 | 2.7037 |
| 0.9973 | 60 | 240 | 55 | 2.3016 | 2.2595 | 1.8287 | 0.3496 | 0.3534 | 1.0918 |
| 0.9754 | 75 | 195 | 12 | 2.3882 | 2.3051 | 3.4780 | 0.4073 | 0.4047 | 0.6264 |
| 1.0719 | 15 | 315 | 23 | 2.4195 | 2.4380 | 0.7654 | 0.4217 | 0.4267 | 1.1863 |
| 1.0592 | 5 | 282 | 45 | 2.3725 | 2.3813 | 0.3703 | 0.3846 | 0.3818 | 0.7355 |
| 1.0946 | 45 | 137 | 63 | 2.3596 | 2.3687 | 0.3839 | 0.3378 | 0.3438 | 1.7855 |
| 1.1123 | 53 | 346 | 10 | 2.8537 | 2.8473 | 0.2226 | 0.5449 | 0.5276 | 3.1723 |

**Directed random search:**

| V | S.A. | L.L. | S.R. | $V_{PSB}$ | $V_{DRS}$ | $error_V$ | $T_{PSB}$ | $T_{DRS}$ | $error_T$ |
|---|---|---|---|---|---|---|---|---|---|
| 0.9491 | 30 | 375 | 40 | 2.3508 | 2.3841 | 1.4160 | 0.3652 | 0.3789 | 3.7515 |
| 0.9127 | 30 | 240 | 40 | 2.2769 | 2.3126 | 1.5693 | 0.3107 | 0.3208 | 3.2584 |
| 0.9973 | 60 | 240 | 55 | 2.3016 | 2.3311 | 1.2804 | 0.3496 | 0.3588 | 2.6342 |
| 0.9754 | 75 | 195 | 12 | 2.3882 | 2.4520 | 2.6723 | 0.4073 | 0.4143 | 1.7246 |
| 1.0719 | 15 | 315 | 23 | 2.4195 | 2.4727 | 2.1976 | 0.4217 | 0.4344 | 3.0100 |
| 1.0592 | 5 | 282 | 45 | 2.3725 | 2.4366 | 2.7019 | 0.3846 | 0.4022 | 4.5693 |
| 1.0946 | 45 | 137 | 63 | 2.3596 | 2.4366 | 3.2650 | 0.3378 | 0.3533 | 4.5744 |
| 1.1123 | 53 | 346 | 10 | 2.8537 | 2.9509 | 3.4046 | 0.5449 | 0.5637 | 3.4563 |

**Quick propagation:**

| V | S.A. | L.L. | S.R. | $V_{PSB}$ | $V_{QP}$ | $error_V$ | $T_{PSB}$ | $T_{QP}$ | $error_T$ |
|---|---|---|---|---|---|---|---|---|---|
| 0.9491 | 30 | 375 | 40 | 2.3508 | 2.3353 | 0.6603 | 0.3652 | 0.3599 | 1.4406 |
| 0.9127 | 30 | 240 | 40 | 2.2769 | 2.2540 | 1.0062 | 0.3107 | 0.3041 | 2.1092 |
| 0.9973 | 60 | 240 | 55 | 2.3016 | 2.3089 | 0.3189 | 0.3496 | 0.3404 | 2.6268 |
| 0.9754 | 75 | 195 | 12 | 2.3882 | 2.4364 | 2.0167 | 0.4073 | 0.3990 | 2.0424 |
| 1.0719 | 15 | 315 | 23 | 2.4195 | 2.3616 | 2.3918 | 0.4217 | 0.4298 | 1.9313 |
| 1.0592 | 5 | 282 | 45 | 2.3725 | 2.4179 | 1.9131 | 0.3846 | 0.3925 | 2.0425 |
| 1.0946 | 45 | 137 | 63 | 2.3596 | 2.3244 | 1.4901 | 0.3378 | 0.3439 | 1.7914 |
| 1.1123 | 53 | 346 | 10 | 2.8537 | 2.9181 | 2.2555 | 0.5449 | 0.5433 | 0.2891 |

**Radial basis function:**

| V | S.A. | L.L. | S.R. | $V_{PSB}$ | $V_{RBF}$ | $error_V$ | $T_{PSB}$ | $T_{RBF}$ | $error_T$ |
|---|---|---|---|---|---|---|---|---|---|
| 0.9491 | 30 | 375 | 40 | 2.3508 | 2.3297 | 0.8994 | 0.3652 | 0.3528 | 3.4043 |
| 0.9127 | 30 | 240 | 40 | 2.2769 | 2.2352 | 1.8313 | 0.3107 | 0.3049 | 1.8626 |
| 0.9973 | 60 | 240 | 55 | 2.3016 | 2.2241 | 3.3692 | 0.3496 | 0.3573 | 2.2156 |
| 0.9754 | 75 | 195 | 12 | 2.3882 | 2.4769 | 3.7151 | 0.4073 | 0.4200 | 3.1263 |
| 1.0719 | 15 | 315 | 23 | 2.4195 | 2.3335 | 3.5548 | 0.4217 | 0.4402 | 4.3773 |
| 1.0592 | 5 | 282 | 45 | 2.3725 | 2.3385 | 1.4334 | 0.3846 | 0.3789 | 1.4749 |
| 1.0946 | 45 | 137 | 63 | 2.3596 | 2.3029 | 2.4033 | 0.3378 | 0.3251 | 3.7701 |
| 1.1123 | 53 | 346 | 10 | 2.8537 | 2.8653 | 0.4048 | 0.5449 | 0.5630 | 3.3258 |

V = voltage at sending end of transmission line before switching [p.u.], S.A. = switching angle [deg.], L.L. = line length [km], S.R. = shunt reactor capacity [MVAR], $V_{PSB}$ = overvoltage peak calculated by PSB [p.u.], $V_{BP}$ = overvoltage peak calculated by BP [p.u.], $V_{DBD}$ = overvoltage peak calculated by BDB [p.u.], $V_{EDBD}$ = overvoltage peak calculated by EBDB [p.u.], $V_{DRS}$ = overvoltage peak calculated by DRS [p.u.], $V_{QP}$ = overvoltage peak calculated by QP [p.u.], $V_{RBF}$ = overvoltage peak calculated by RBF [p.u.], $T_{PSB}$ = overvoltage duration calculated by PSB [s], $T_{BP}$ = overvoltage duration calculated by BP [s], $T_{DBD}$ = overvoltage duration calculated by BDB [s], $T_{EDBD}$ = overvoltage duration calculated by EBDB [s], $T_{DRS}$ = overvoltage duration calculated by DRS [s], $T_{QP}$ = overvoltage duration calculated by QP [s], $T_{RBF}$ = overvoltage duration calculated by RBF [s], $error_V$ = voltage error [%], $error_T$ = duration time error [%], Phase = phases that have maximum overvoltages.

6) Repeat Steps 1 to 5 with various system parameters to learn artificial neural network.
7) Test the artificial neural network with different system parameters.

3.3. **Study of transmission lines energization.** In most countries, the main step in the process of power system restoration, following a complete/partial blackout is energization of primary restorative transmission lines. Switching overvoltage is primary important in insulation co-ordination for extra high voltage (EHV) lines. The objective of simulating switching overvoltage is to help for a proper insulation co-ordination and would lead to minimize damage and interruption to service as a consequence of steady state, dynamic and transient overvoltage [30].

During the early stages of restoring high voltage overhead and underground transmission lines, concerns are with three related overvoltages: sustained power frequency overvoltages, switching transients (surges), and harmonic resonance. In the early stages of the restoration, the lines are lightly loaded; resonance therefore is lightly damped, which in turn means the resulting resonance voltages may be very high [1]. In order to reduce the steady state overvoltage of no load transmission lines, a shunt reactor is connected at the receiving end of transmission line.

Unlike [15], three-phase transmission lines are studied in this paper. Also, equivalent parameters of the network are adopted as ANN inputs; therefore there is no need to train an ANN for every studied system.

In practical system, a number of factors affect the overvoltages factors due to energization or reclosing. In this paper following parameters are considered:

- Voltage at the sending-end bus of the transmission line before switching
- Equivalent resistance of the network
- Equivalent inductance of the network
- Equivalent capacitance of the network
- Closing time of the circuit breaker poles
- Line length
- Line capacitance
- Shunt reactor capacity

The steps for transient overvoltages estimation are listed below:

1) Determine the characteristics of transmission line that should be energized.
2) Run PSB simulation.
3) Determine the overvoltage peak and duration.
4) Repeat Steps 1 to 3 with various system parameters to learn artificial neural network.
5) Test the artificial neural network with different system parameters.

4. **Case Study.** In this section, the proposed algorithm is demonstrated for three case studies that are a portion of 39-bus New England test system which are shown in Figure 6, and its parameters are listed in [31].

The electrical components of the network are modeled using the MATLAB/Simulink environment [32,33]. These models should be adapted for the desired frequency range (here the frequencies up to $f = 10f_0$ are considered to be sufficient). The generator is represented by an ideal voltage source behind the sub-transient inductance in series with the armature winding resistance that can be as accurate as the Park model [34]. Phase of voltage source is determined by the load flow results. Transmission lines are described by distributed line models. The circuit breaker is represented by an ideal switch. The transformer model takes into account the winding resistances ($R_1, R_2$), the leakage inductances ($L_1, L_2$) as well as the magnetizing characteristics of the core, which is modeled by a resistance, $R_m$, simulating the core active losses and a saturable inductance,

TABLE 6. Average of relative and absolute errors for various ANN models

| ANN model | Average of relative peak error [%] | Average of absolute peak error [p.u.] | Average of relative duration time error [%] | Average of absolute duration time error [s] |
|---|---|---|---|---|
| **Transformer Energization:** | | | | |
| BP | 1.6865 | 0.0266 | 1.6934 | 0.0069 |
| DBD | 1.8883 | 0.0297 | 1.7708 | 0.0064 |
| EDBD | 1.3928 | 0.0231 | 1.1141 | 0.0037 |
| DRS | 2.8476 | 0.0478 | 2.7579 | 0.0114 |
| QP | 1.4176 | 0.0243 | 1.2989 | 0.0055 |
| RBF | 2.3779 | 0.0380 | 2.2122 | 0.0087 |
| **Shunt Reactor Energization:** | | | | |
| **ANN model** | **Average of relative peak error [%]** | **Average of absolute peak error [p.u.]** | **Average of relative duration time error [%]** | **Average of absolute duration time error [s]** |
| BP | 1.6841 | 0.0321 | 1.9617 | 0.0094 |
| DBD | 1.8359 | 0.0359 | 2.0771 | 0.0090 |
| EDBD | 1.2134 | 0.0213 | 1.5923 | 0.0074 |
| DRS | 3.0144 | 0.0555 | 2.6923 | 0.0122 |
| QP | 1.5393 | 0.0261 | 1.8577 | 0.0084 |
| RBF | 2.1935 | 0.0397 | 2.5188 | 0.0105 |
| **Transmission Line Energization:** | | | | |
| **ANN model** | **Average of relative peak error [%]** | **Average of absolute peak error [p.u.]** | **Average of relative duration time error [%]** | **Average of absolute duration time error [s]** |
| BP | 1.5412 | 0.0374 | 1.9901 | 0.0077 |
| DBD | 1.7605 | 0.0430 | 2.0836 | 0.0083 |
| EDBD | 1.4345 | 0.0338 | 1.6565 | 0.0066 |
| DRS | 2.3134 | 0.0567 | 3.3723 | 0.0131 |
| QP | 1.5066 | 0.0371 | 1.7842 | 0.0066 |
| RBF | 2.2014 | 0.0522 | 2.9446 | 0.0117 |

$L_{sat}$. The shunt reactor model takes into account the leakage inductance as well as the magnetizing characteristics of the core, which is modeled by a resistance, $R_m$, simulating the core active losses and a saturable inductance, $L_{sat}$. The saturation characteristic is specified as a piece-wise linear characteristic [28]. All of the loads are modeled as constant impedances.

Figure 6(a) shows a one-line diagram of a portion of 39-bus New England test system which is in restorative state. The generator at bus 35 is a black-start unit. The load 19 shows cranking power of the later generator that must be restored by the transformer of bus 19. When the transformer is energized, harmonic overvoltages can be produced because the transformer is lightly loaded. The equivalent circuit of this system that seen behind bus 16 is determined and values of equivalent resistance, equivalent inductance, and equivalent capacitance are calculated. In other words, the case study system is converted to equivalent system of Figure 3(a). Values of equivalent resistance, equivalent inductance and equivalent capacitance are 0.00326 p.u., 0.02793 and 1.8561 p.u., respectively. For testing trained ANN, values of voltage at transformer bus (bus 19) and line length are varied and overvoltage peak and duration are calculated using developed ANN.

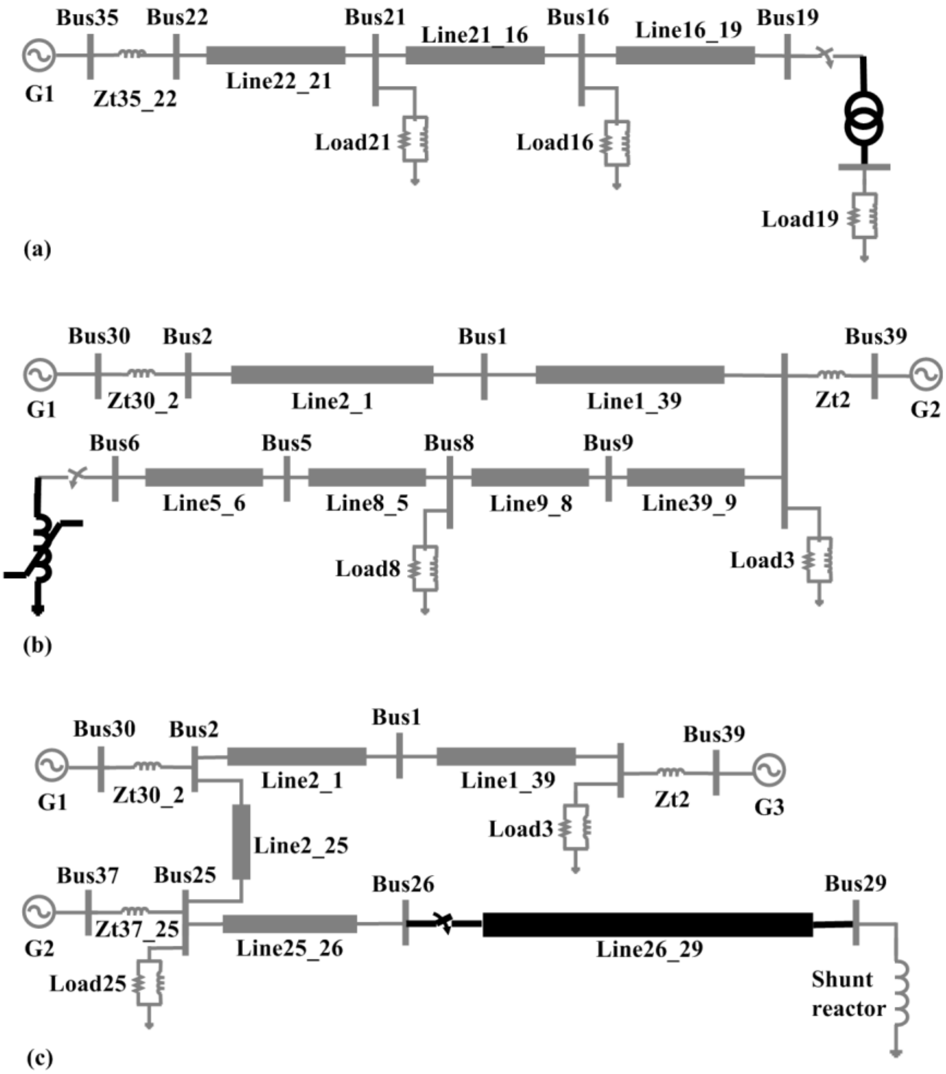


Figure 6. Portions of 39-bus New England test system. (a) Transformer energization, (b) shunt reactor energization, and (c) transmission line energization.

Table 3 contains the some sample result of test data of transformer energization for BP, DBD, EDBD, DRS, QP and RBF.

As another example, the system in Figure 6(b) is examined. In the next step of the restoration, unit at bus 6 must be restarted. In order to reduce the steady state overvoltage of no load transmission lines, the reactor at bus 6 should be energized. In this condition, harmonic overvoltages can be produced. After calculating equivalent circuit seen from bus 5, various cases of shunt reactor energization are taken into account and corresponding overvoltages peak and duration are computed from PSB program and trained ANN. In this case, values of equivalent resistance, equivalent inductance and equivalent capacitance are 0.00577 p.u., 0.02069, and 0.99 p.u., respectively. Summary of a few results is presented in Table 4 for BP, DBD, EDBD, DRS, QP and RBF.

For testing developed ANN for transmission lines energization study, the system in Figure 6(c) is examined that is another portion of 39-bus New England test system. In the next step of the restoration, line 26_29 must be restarted. As mentioned before, first this system is converted to equivalent circuit of Figure 3(c). In this case, values of equivalent resistance, equivalent inductance and equivalent capacitance are 0.00792 p.u., 0.0247, and

1.1594 p.u., respectively. For testing developed ANN, various cases of transmission line energization are taken into account and corresponding peak and duration of overvoltages are computed from PSB program and trained ANN. Summary of a few results is presented in Table 5 for BP, DBD, EDBD, DRS, QP and RBF.

5. **Discussion.** In this paper, switching overvoltages are evaluated using BP, DBD, EDBD, DRS, QP and RBF. As can be seen in Tables 3-5, all trained ANNs can estimate overvoltages peak and duration with proper accuracy. To select best approach for overvoltages evaluation, a comparison has been made. Table 6 presents a comparison between these methods based on average of relative and absolute errors. BP and RBF are the most common structures to train ANNs in the literature. However, it can be seen from Table 6 that EDBD algorithm has better performance (smaller relative and absolute errors) to evaluate switching overvoltages in the power system restoration studies.

6. **Conclusion.** The study has successfully presented a novel approach based on ANN to evaluate and control the switching overvoltages. Six ANN models including backpropagation, delta-bar-delta, extended delta-bar-delta, directed random search, quick propagation, and radial basis function are adopted to train ANN. ANN Training is performed using equivalent circuit parameters of the network to achieve good generalization capability for developed ANN. The results from this scheme are close to results from the conventional method and can assist prediction of the overvoltage of other case studies within the range of training set. Proposed method for transformer and shunt reactor energization study, omits time-consuming time-domain simulations and it is suitable for real time applications during system restoration. The developed ANN approach is tested on a partial 39-bus New England test system for transformer, shunt reactor, and transmission line energization and results show that EDBD algorithm presents best performance. This approach is recommended as an operator-training tool for estimation of switching overvoltages during power system restoration.

## REFERENCES


[1] M. M. Adibi, R. W. Alexander and B. Avramovic, Overvoltage control during restoration, *IEEE Trans. on Power Syst.*, vol.7, no.4, pp.1464-1470, 1992.

[2] A. Ketabi, A. M. Ranjbar and R. Feuillet, Analysis and control of temporary overvoltages for automated restoration planning, *IEEE Trans. on Power Delivery*, vol.17, no.4, pp.1121-1127, 2002.

[3] I. Sadeghkhani and A. Ketabi, *Switching Overvoltages During Restoration: Evaluation and Control Using ANN*, Lambert Academic Publishing, 2012.

[4] T. Hayashi et al., Modeling and simulation of black start and restoration of an electric power system. Results of a questionnaire, *Electra*, no.131, pp.157-169, 1990.

[5] S. A. Taher and I. Sadeghkhani, Estimation of magnitude and time duration of temporary overvoltages using ANN in transmission lines during power system restoration, *Simulation Modelling Practice and Theory*, vol.18, no.6, pp.787-805, 2010.

[6] X. Liu, X. Cui and L. Qi, Calculation of lightning-induced overvoltages on overhead lines based on DEPACT Macromodel using circuit simulation software, *IEEE Trans. on Electromagnetic Compatibility*, vol.54, no.4, pp.837-849, 2012.

[7] B. Gustavsen, Study of transformer resonant overvoltages caused by cable-transformer high-frequency interaction, *IEEE Trans. on Power Delivery*, vol.25, no.2, pp.770-779, 2010.

[8] G. Morin, Service restoration following a major failure on the hydroquebec power system, *IEEE Trans. on Power Delivery*, vol.2, no.2, pp.454-463, 1987.

[9] A. Ketabi, I. Sadeghkhani and R. Feuillet, Using artificial neural network to analyze harmonic overvoltages during power system restoration, *European Trans. on Electrical Power*, vol.21, no.7, pp.1941-1953, 2011.

[10] V. Jankov, Estimation of the maximal voltage induced on an overhead line due to the nearby lightning, *IEEE Trans. on Power Delivery*, vol.12, no.1, pp.315-324, 1997.

[11] V. Cooray, Calculating lightning-induced overvoltages in power lines. A comparison of two coupling models, *IEEE Trans. on Electromagnetic Compatibility*, vol.36, no.3, pp.179-182, 1994.
[12] S. Yanabu, H. Murase, H. Aoyagi, H. Okubo and Y. Kawaguchi, Estimation of fast transient overvoltage in gas-insulated substation, *IEEE Trans. on Power Delivery*, vol.5, no.4, pp.1875-1882, 1990.
[13] L. M. Wedepohl and D. J. Wilcox, Estimation of transient sheath overvoltages in power-cable transmission systems, *Proc. of Inst. Elect. Eng.*, vol.120, no.8, pp.877-882, 1973.
[14] M. Shafiee, B. Vahidi, S. H. Hosseinian and S. Jazebi, Using artificial neural network to estimate maximum overvoltage on cables with considering forward and backward waves, *The 43rd International Universities Power Engineering Conference – UPEC*, 2008.
[15] D. Thukaram, H. P. Khincha and S. Khandelwal, Estimation of switching transient peak overvoltages during transmission line energization using artificial neural network, *Electric Power System Research*, vol.76, no.4, pp.259-269, 2006.
[16] I. Sadeghkhani and A. Mortazavian, Analysis of transformer harmonic overvoltages during power system restoration, *Advances in Electrical Engineering Systems*, vol.1, no.1, pp.49-53, 2012.
[17] C. Yildiz, S. Gultekin, K. Guney and S. Sagiroglu, Neural models for the resonant frequency of electrically thin and thick circular microstrip antennas and the characteristic parameters of asymmetric coplanar waveguides backed with a conductor, *AEU – International Journal of Electronics and Communications*, vol.56, no.6, pp.396-406, 2002.
[18] S. Haykin, *Neural Network: A Comprehensive Foundation*, 2nd Edtition, Prentice Hall, 1998.
[19] R. Bayindir, S. Sagiroglu and I. Colak, An intelligent power factor corrector for power system using artificial neural networks, *Electric Power Systems Research*, vol.79, no.1, pp.152-160, 2009.
[20] S. Bunjongjit and A. Ngaopitakkul, Selection of proper artificial neural networks for fault classification on single circuit transmission line, *International Journal of Innovative Computing, Information and Control*, vol.8, no.1(A), pp.361-374, 2012.
[21] I.-T. Chen, J.-T. Tsai, C.-F. Wen and W.-H. Ho, Artificial neural network with hybrid Taguchi-Genetic algorithm for nonlinear MIMO model of machining processes, *International Journal of Innovative Computing, Information and Control*, vol.9, no.4, pp.1455-1475, 2013.
[22] R. A. Jacobs, Increased rate of convergence through learning rate adaptation, *Neural Networks*, vol.1, no.4, pp.295-307, 1988.
[23] A. Minai and R. D. Williams, Acceleration of backpropagation through learning rate and momentum adaptation, *Proc. of International Joint Conference on Neural Networks*, pp.676-679, 1990.
[24] J. Matyas, Random optimization, *Automation and Remote Control*, vol.26, no.2, pp.246-253, 1965.
[25] S. E. Fahlman, Fast learning variations on back propagation: An empirical study, *Proc. of the 1988 Connectionist Models Summer School*, pp.38-51, 1988.
[26] A. Karami and M. S. Mohammadi, Radial basis function neural network for power system load-flow, *International Journal of Electrical Power & Energy Systems*, vol.30, no.1, pp.60-66, 2008.
[27] P. K. Dash, A. K. Pradhan and G. Panda, Application of minimal radial basis function neural network to distance protection, *IEEE Trans. on Power Deliv.*, vol.16, no.1, pp.68-74, 2001.
[28] G. Sybille, M. M. Gavrilovic, J. Belanger and V. Q. Do, Transformer saturation effects on EHV system overvoltages, *IEEE Trans. on Power App. Syst.*, vol.PAS-104, no.3, pp.671-680, 1985.
[29] L. Prikler, G. Ban and G. Banfai, EMTP models for simulation of shunt reactor switching transients, *International Journal of Electrical Power & Energy Systems*, vol.19, no.4, pp.235-240, 1997.
[30] T. Keokhoungning, S. Premrudeepreechacharn and K. Ngamsanroaj, Evaluation of switching overvoltage in 500 kV transmission line interconnection Nam Theun 2 power plant to Roi Et 2 substation, *Proc. of Asia Pacific Power and Energy Engineering Conference*, pp.1-4, 2009.
[31] S. Wunderlich, M. M. Adibi, R. Fischl and C. O. D. Nwankpa, An approach to standing phase angle reduction, *IEEE Trans. on Power Syst.*, vol.9, no.1, pp.470-478, 1994.
[32] A. Ketabi and I. Sadeghkhani, *Electric Power Systems Simulation Using MATLAB*, 2nd Edition, Morsal Publications, 2012 (in Persian).
[33] G. Sybille, P. Brunelle, L. Hoang, L. A. Dessaint and K. Al-Haddad, Theory and applications of power system blockset, a MATLAB/Simulink-based simulation tool for power systems, *Proc. of IEEE Power Eng. Soc. Winter Meeting*, vol.1, pp.774-779, 2000.
[34] M. M. Duro, Damping modelling in transformer energization studies for system restoration: Some standard models compared to field measurements, *Proc. of IEEE Bucharest Power Tech Conference*, Bucharest, Romania, 2009.